Numerical simulation on the maximum temperature and smoke back-layering length in a tilted tunnel under natural ventilation

Xiaolei Zhang[a*], Yujie Lin[a], Congling Shi[b*], Jianping Zhang[c]

[a] State Key Laboratory of Fire Science,
University of Science and Technology of China,
Hefei, Anhui, 230026, China

[b] Beijing Key Laboratory of Metro Fire and Passenger Transportation Safety,
China Academy of Safety Science and Technology,
Beijing, 100012, China

[c] FireSERT, School of Built Environment,
Ulster University, Newtownabbey, BT37 0QB, Northern Ireland, UK

*Corresponding author: Email address: zxlcjc@ustc.edu.cn; Postal address: State Key Laboratory of Fire Science, University of Science and Technology of China, Hefei, Anhui, 230026, PR China (X.L. Zhang).

Email address: shicl@chinasafety.ac.cn; Postal address: Beijing Key Laboratory of Metro Fire and Passenger Transportation Safety, China Academy of Safety Science and Technology, Beijing 100012, PR China (C.L. Shi).

Abstract

The present study investigates the maximum temperature and smoke back-layering length *S* in the downhill direction from the fire source in a tilted tunnel under natural ventilation. Numerical simulations were conducted using FDS to study the smoke flow behaviors for a fire in a tunnel with nine tunnel slopes of 0, 1%, 2%, 3%, 4%, 5%, 6%, 7% and 8%. It was found that, due to the stack effect, the smoke stagnated at a distance from the fire source in the downhill direction. The effects of tunnel slope, α, fire source heat release rate, $\dot{Q}$, source-ceiling height *H* and tunnel width *W* on the maximum temperature and smoke back-layering length were studied. Results showed that the maximum temperature under the ceiling decreased with the increasing of tunnel slope or the decreasing of tunnel width. However, it increased with the increasing of heat release rate or the decreasing of source-ceiling height. A model was proposed for the maximum temperature rise. The smoke back-layering length *S* decreased with the increasing of the tunnel slope. Fire source heat release rate and tunnel width had no significant effect on the smoke back-layering length. And the smoke back-layering length decreased with the decreasing of source-ceiling height. Based on dimensional analysis, a simple model including the effects of both the tunnel slope and source-ceiling height *H*, was proposed to predict the smoke back-layering length.

Key words: Tunnel fire; tunnel slope; smoke back-layering length; temperature; FDS.

Nomenclature

$b_{f,0}$	area-equivalent radius (m)
c_p	specific heat of air at constant pressure ($kJkg^{-1}K^{-1}$)
D^*	characteristic fire diameter as shown in Eq. (5) (m)
g	gravitational acceleration (ms^{-2})
h	the thickness of the smoke layer at the stagnation point (m)
H	source-ceiling height (m)

H_t	tunnel height (m)
k	constant in Eq. (16)
$\dot{Q}$	total heat release rate (kW)
$\dot{Q}^*$	non-dimensional heat release rate (Eq. (2b))
r	distance from the fire source (m)
S	smoke back-layering length (m)
T_{max}	maximum smoke temperature under the ceiling (K)
Ts	smoke temperature at the smoke stagnation point (K)
T_x	mean temperature at the distance x from the reference point (K)
T_∞	ambient temperature (K)
V	longitudinal ventilation velocity (ms^{-1})
V'	non-dimensional ventilation velocity (Eq. (1))
V^*	non-dimensional ventilation velocity (Eq. (2c))
W	tunnel width (m)
Greek symbols	
α	tunnel slope (%)
ρ_s	smoke density at the smoke stagnation point (kgm^{-3})
ρ_x	smoke density at the distance x from the reference point (kgm^{-3})
ρ_∞	ambient air density (kgm^{-3})
ΔP_{stack}	pressure difference caused by the stack effect ($kgm^{-1}s^{-2}$)
ΔP_{static}	static pressure difference ($kgm^{-1}s^{-2}$)
ΔT_{max}	maximum temperature rise (K)
ΔT_r	temperature rise of the reference point at location of x_r (K)
ΔT_s	temperature rise at the smoke stagnation point (K)
ΔT_x	temperature rise at the distance x from the reference point (K)
$\Delta\rho_s$	density difference between ambient air and the smoke stagnation point (kgm^{-3})
δ	mesh size (m)
θ	tunnel inclination angle (°)
$\Pi_1, \Pi_2, \Pi_3, \Pi_4,$ Π_5, Π_6	non-dimensional quantities
Subscript	
∞	ambient

1. Introduction

Smoke temperature and back-layering length are two of the most important parameters in tunnel fires, and have been studied for decades. Most of the previous studies on the temperature profile and smoke back-layering length of tunnel fires were focused on a horizontal tunnel (Chen *et al.*, 2013, 2015; Hu *et al.*, 2003, 2005, 2007, 2008; Kurioka *et al.*, 2003; Li and Ingason, 2010, 2011, 2012; Tang *et al.*, 2013; Tang *et al.*, 2014). For the temperature profile under the ceiling of tunnel fires, Li and Ingason, 2011, 2012 proposed a widely used correlation for calculating the maximum temperature rise $\Delta T_{\max}$ under the ceiling, as shown in Eq. (1) where two regions were defined based on a dimensionless ventilation velocity.

Region I ($V' = V \Big/ \left(\frac{g\dot{Q}}{b_{f0}\rho_\infty c_p T_\infty} \right)^{1/3} \le 0.19$)

$$\Delta T_{\max} = \begin{cases} 17.5\frac{\dot{Q}^{2/3}}{H^{5/3}}, 17.5\frac{\dot{Q}^{2/3}}{H^{5/3}} < 1350 \\ 1350, \quad 17.5\frac{\dot{Q}^{2/3}}{H^{5/3}} \ge 1350 \end{cases} \tag{1a}$$

Region II ($V' > 0.19$)

$$\Delta T_{\max} = \begin{cases} \frac{\dot{Q}}{Vb_{f0}^{1/3}H^{5/3}}, \frac{\dot{Q}}{Vb_{f0}^{1/3}H^{5/3}} < 1350 \\ 1350, \quad \frac{\dot{Q}}{Vb_{f0}^{1/3}H^{5/3}} \ge 1350 \end{cases} \tag{1b}$$

V is the longitudinal ventilation velocity, $\dot{Q}$ is the heat release rate, ρ_∞ is the ambient air density, c_p is the specific heat of air at constant pressure, g is the gravitational acceleration, T_∞ is the ambient air temperature, $b_{f,0}$ is the area-equivalent radius, and H is the source-ceiling height. For smoke back-layering length S of a horizontal tunnel with logitudinal ventilation, the follwing corrleation was proposed (Li and Ingason, 2010):

$$\frac{S}{H}=\begin{cases}18.5\ln\left(0.81\dot{Q}^{*1/3}/V^{*}\right), \dot{Q}^{*}\le 0.15\\ 18.5\ln\left(0.43/V^{*}\right), \quad \dot{Q}^{*}>0.15\end{cases} \tag{2a}$$

where

$$\dot{Q}^{*}=\frac{\dot{Q}}{\rho_{\infty}c_{p}T_{\infty}\sqrt{g}H^{5/2}} \tag{2b}$$

$$V^{*}=\frac{V}{\sqrt{gH}} \tag{2c}$$

It should be noted that, for a horizontal tunnel under natural ventilation, smoke will spread out of the tunnel from both ends of the tunnel, and therefore there is no smoke back-layering length.

In real situations, there will be slopes in some tunnels. The stack effect of a titled tunnel has an important influence on smoke spread, which will further change the maximum temperature under the ceiling and smoke back-layering length, and some studies have been conducted on these two parameters of a tilted tunnel (Atkinson and Wu, 1996; Chow *et al.*, 2015; Hu *et al.*, 2013; Oka *et al.*, 2013; Shafee and Yozgatligil, 2018; Weng *et al.*, 2016; Wu *et al.*, 1997). For maximum temperature, on the basis of Li's study (Eq. (1)), Hu *et al.*, 2013 proposed the following equation based on experimental results using a small-scale tunnel model

$$\Delta T_{\max}=\begin{cases}\left(1-0.067\alpha\right)\dfrac{\dot{Q}^{2/3}}{Vb_{f,0}{}^{1/3}H^{5/3}}, V'>0.19\\ \left(1-0.061\alpha\right)17.5\dfrac{\dot{Q}^{2/3}}{H^{5/3}}, \quad V'\le 0.19\end{cases} \tag{3}$$

For the smoke back-layering, Atkinson and Wu, 1996, Wu *et al.*, 1997 conducted experiments using a small-scale tilted tunnel with various slopes, and the velocities to prevent smoke back-layering to various distances in the uphill direction from the fire source were obtained, and a correlation was developed for the critical velocity that was just able to prevent the formation of smoke back-layering length *S*. Chow *et al.*, 2015 also performed experiments using a small-scale tilted tunnel with various

slopes, and an equation of critical velocity for S=0 in the uphill direction from the fire source was further proposed which was similar to that proposed in (Atkinson and Wu, 1996; Wu *et al.*, 1997). Shafee and Yozgatligil, 2018 carried out experiments using a reduced-scale tilted tunnel model, and S of various ventilation velocities in the uphill direction from the fire source were obtained, and a correlation of critical velocity was also developed for S=0. Recently, Weng *et al.*, 2016 proposed a theoretical model of the critical velocity for both uphill and downhill direction from the fire source based on non-dimensional analysis, and they found that the non-dimensional critical velocity was a 1/3 power function of the non-dimensional heat release rate and proportional to the tunnel slope.

The results in the above studies show that due to stack effect, the smoke movement in a tilted tunnel is different from the one in a horizontal tunnel. The specific smoke movements of tilted tunnel fires would make the maximum temperature and smoke back-layering length different from those of horizontal tunnel fires. Unfortunately, previous studies are mainly conducted with longitudinal ventilation, and little effort has been put with respect to the maximum temperature and smoke back-layering length of tilted tunnel with the absence of mechanical ventilation. The smoke movement will be dominated by the airflow induced by stack effect, and even for natural ventilation (when the ventilation system isn't working) there would be smoke back-layering length in the downhill direction. Most of the models proposed in previous studies for longitudinal ventilation cannot be applied for any more (Ji *et al.*, 2015). Oka *et al.*, 2013 proposed the following equation for smoke back-layering length in the downhill direction based on data obtained from a small-scale tilted tunnel test under natural ventilation

$$\frac{S}{\dot{Q}^{2/5}} = 3.18\theta^{-0.562} \tag{4}$$

where θ is the tunnel inclination angle (°). However, they have only examined two small heat

release rates (1.95 and 5.78 KW) in a small-scale tunnel (1/23.3-scale model tunnel), thus, the viability of the model proposed by them needs further validations for other conditions. In this work, numerical simulation is conducted for the maximum temperature and smoke back-layering length in a tilted tunnel under natural ventilation. The tunnel length is 500 m, and the tunnel height is set to be 5 m. The tunnel width is varied in the range of 6 m ~ 12 m. The evolution behaviors of maximum temperature and smoke back-layering length for various slopes, heat release rates, source-ceiling heights and tunnel widths are studied.

2. CFD modeling

2.1 The physical model

In order to study the smoke back-layering length in the lower end of the tilted tunnel under natural ventilation, the total length of the tilted tunnel is set to be 500 m. The cross section of the tunnel is rectangular with height of 5 m, and the width of the tunnel is varied from 6 m to 12 m. The fire source is located at 350 m from the portal in the lower end as shown in Fig. 1 (on the longitudinal axis of the tunnel), and heptane is used as the fuel. The default values in FDS User Guide are used for the fire source (Fire Dynamics Simulator User's Guide). The turbulence model is "constant Smagorinsky". The simple chemistry, mixing-controlled combustion model (single-step) is used for the reaction, and specify energy release per unit mass oxygen of 1.31×10^4 kJ/kg. The material of the wall is specified as concrete with its thermal properties (conductivity is 1.8 W/(mK), density is 2280 kg/m^3, specific heat is 1.04 kJ/(kgK)) available in the FDS (Version: 6.5.3) database document. The ambient temperature was 20°C, and the environmental pressure was set as ambient pressure of 101 kPa. The two ends of the tunnel are set to be open. All the simulation conditions are shown in Table 1. Two heat release rates (*HRR*), three source-ceiling heights (*H*), three tunnel widths

(W) and nine slopes α (%) are used. The heat release rates of 5 MW and 7.5 MW are considered to simulate a common fire scenario of one passenger car burning (Ko *et al.*, 2010). For the effect of tunnel slope on the smoke temperature and back-layering length, nine slopes are considered. Considering the computational power and economy, for various heat release rates, source-ceiling heights and tunnel widths, tunnel slopes of 0, 1%, 2%, 4%, 6% and 8% are used in this study. The tunnel slope is obtained by decomposing the acceleration of gravity in the tunnel longitudinal direction and the tunnel height direction. For example, a slope of 8% is obtained by setting the acceleration of gravity in the tunnel longitudinal direction as $\frac{g}{\sqrt{1.0064}}$ and the acceleration of gravity in the tunnel height direction as $0.08\frac{g}{\sqrt{1.0064}}$. The simulation time is set to be 1200 s to reach a steady spread state of the smoke. Multiple mesh simulation with MPI parallel processing (number of MPI processes is 5, and number of OpenMP threads is 3) is used during the study. A series of thermocouples are used to measure the temperatures, and the distances between the thermocouples and the ceiling are set to be 0.1 m, 0.225 m, 0.35 m, 0.6 m, 0.85 m, 1.1 m, 1.6 m, 2.1 m.

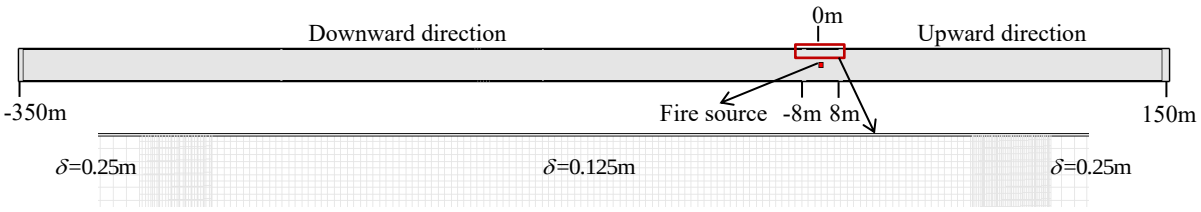

Fig. 1: Physical model of the tilted tunnel and the mesh sizes (top view).

Table 1 Summary of numerical simulation conditions.

Test no.	$\dot{Q}$ (MW)	W (m)	H (m)	α (%)	Test no.	$\dot{Q}$ (MW)	W (m)	H (m)	α (%)
1	5	12	5	0	17	5	12	3	2
2	5	12	5	1	18	5	12	3	4
3	5	12	5	2	19	5	12	3	6

4	5	12	5	3	20	5	12	3	8
5	5	12	5	4	21	5	12	2	1
6	5	12	5	5	22	5	12	2	2
7	5	12	5	6	23	5	12	2	4
8	5	12	5	7	24	5	12	2	6
9	5	12	5	8	25	5	12	2	8
10	7.5	12	5	0	26	5	9	5	1
11	7.5	12	5	1	27	5	9	5	2
12	7.5	12	5	2	28	5	9	5	4
13	7.5	12	5	4	29	5	9	5	6
14	7.5	12	5	6	30	5	9	5	8
15	7.5	12	5	8	31	5	6	5	2
16	5	12	3	1	32	5	6	5	4

2.2 The grid system

For a numerical simulation, mesh size is an important factor to obtain viable results. For simulations involving buoyant plumes, the mesh size δ near the fire is determined by a non-dimentional expression D^*/δ (Chen *et al.*, 2015), where D^* is a characteristic fire diameter as shown in Eq. (5)

$$D^* = \left(\frac{\dot{Q}}{\rho_\infty c_p T_\infty \sqrt{g}} \right)^{2/5} \tag{5}$$

For the heat release rates of the present study (Table 1), D^* is in the range of 1.83 m ~ 2.15 m. According to the studies in the literatures, the value of D^*/δ should be 4 ~ 16 (Shafee and Yozgatligil, 2018; Wang *et al.*, 2019). Therefore, the mesh size of δ is in the range of 0.11 m ~ 0.54 m. Then, the mesh size is set to be 0.125 m near the fire source (8 m from the fire center in both the downhill direction and uphill direction), and 0.25 m in other places as shown in Fig. 1, and the number of mesh for each condition is in the range of 1836000 (W=6 m) ~ 3304800 (W=12 m). It is noted that many numerical studies have been carried out using FDS for a full scale tunnel fire (Harish and Venhatasubbaiah, 2014; Meng *et al.*, 2014; Shafee and Yozgatligil, 2018; Wang *et al.*, 2016; Weng *et al.*, 2016), and similar mesh size were used in these studies with the accuracy

valadited by mesh size sensitivity analysis and comparison with experimental results (Oka *et al.*, 2013; Wu *et al.*, 1997).

In this work, mesh size sensitivity analysis and validation of the FDS prediction have also been conducted, and numerical simulation with smaller mesh size has been carried out. Figure 2a shows a typical comparison between two mesh systems (the number of mesh increases from 2570400 to 4590000) for $\dot{Q}=5\mathrm{MW}$, W=9 m, H=5 m, α=2%. Figure 2a shows that there is no significant difference of maximum temperature betwwen the two mesh systems. For the larger mesh size (near fire source δ=0.125m, other places δ=0.25m), it takes about 9 days with 5 MPI processes for one case. For the smaller mesh size (near fire source δ=0.1m, other places δ=0.2m), we have to use 21 MPI processes to save time, and even so, it takes about 6 days for one case. Considering saving time and resources, the mesh size is set to be 0.125 m near the fire source, and 0.25 m in other places. Figure 2b shows the comparison of temperature rise between this study and the model proposed in Hu, 2006 for horizontal tunnel fire. ΔT_x is the temperature rise at the distance x-x_r from the reference point. ΔT_r is the temperature rise of the reference point at location of x_r. It is noted that in Hu's model, ΔT_x and ΔT_r are mean smoke temperature rise of the transverse section. Figure 2b shows that the FDS predictions match well with Hu's model which is validiated by full scale experimental results.

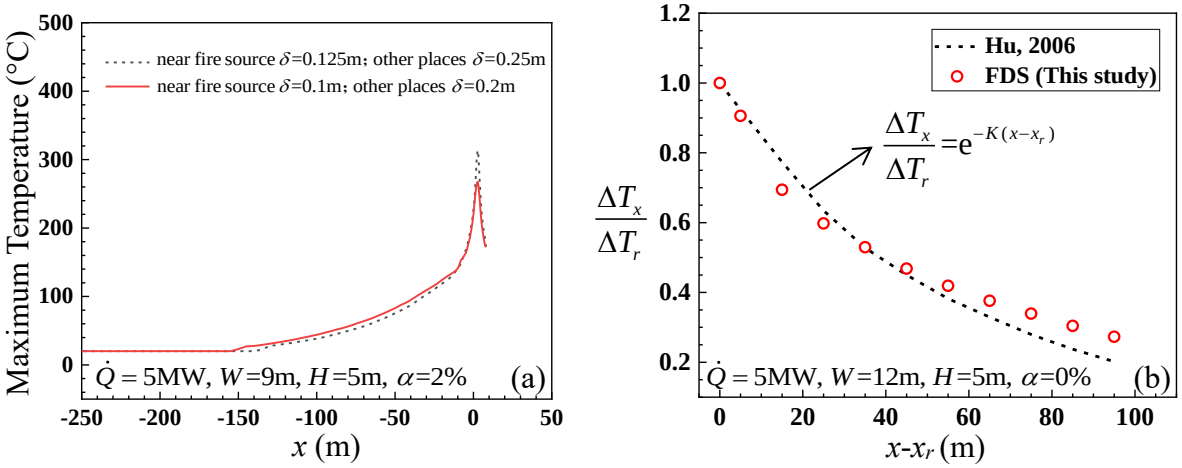

Fig. 2: Validation of the FDS prediction.

3. Results and discussion

Figure 3 shows the typical smoke spread behavior of 7.5 MW, W=12 m, H=5 m and α=2%. It can be seen that after 320 s, it reaches steady spread state and the smoke back-layering in the downhill direction from the fire source has no significant change anymore. The maximum temperature and the smoke back-layering length reported in the following sections are the averaged values in the steady spread state. The simulation results show good repeatability.

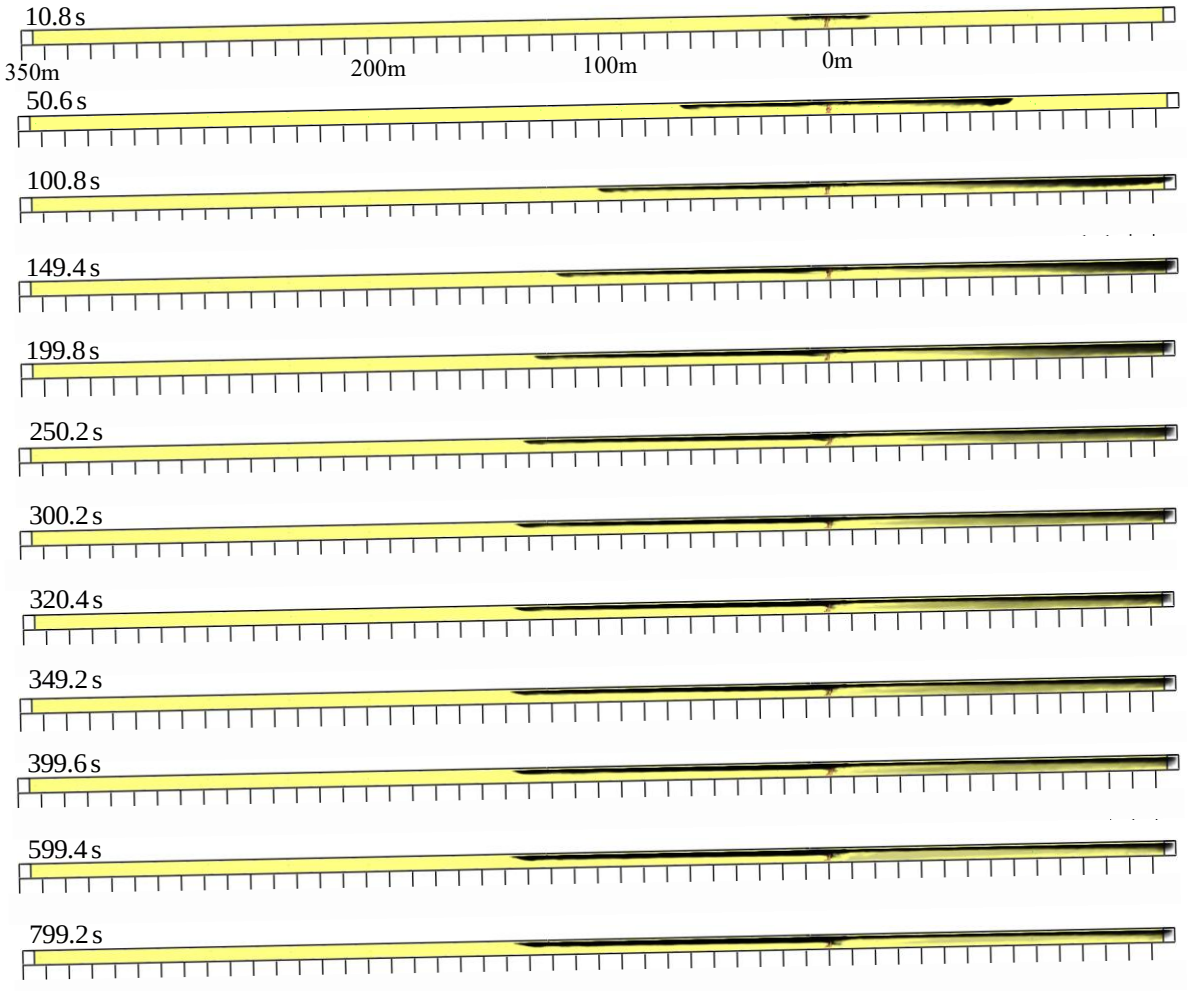

Fig. 3: Smoke spread behavior for 7.5 MW, W=12 m, H=5 m and α=2%.

3.1 Maximum temperature rise under the ceiling

Figures 4 ~ 6 show the maximum temperature T_{max} and temperature rise ΔT_{max} (average value of 50 s over the steady state) of the fire plume under the ceiling with various tunnel slopes, heat release rates, source-ceiling heights and tunnel widths. In order to give a better visualization of the

results plotted at Fig. 4a, Fig. 5a and Fig. 6a, only some slopes are shown in these figures. From Fig. 4, we can see that the maximum temperature decreases with the increasing of the tunnel slope. Wang *et al.*, 2020 and Chen *et al.*, 2020 point out that the air flow velocity induced by the stack effect increases with the tunnel slope. The fire plume will be deflected by the air flow (Hu, 2017) induced by the stack effect. At the same time, the airflow enhances the entrainment of gas. It is also noted that with the increasing of the tunnel slope, the distance from the fire source to the tunnel ceiling above the fire is increased, which results in a decrease in the maximum temperature. Figure 5 also shows that the maximum temperature increases with the increasing of heat release rate and the decreasing of source-ceiling height. The above results are consistent with the experimental results in (Hu *et al.*, 2013). However, the correlation proposed in (Hu *et al.*, 2013) (Eq. (3)) can't predict the decrease in the maximum temperature with decreasing tunnel width as shown in Fig. 6. It is noted that only one tunnel width is used in (Hu *et al.*, 2013), and the effect of tunnel width is not included in their model. The decreasing tunnel width increases the smoke thickness as well as the heat transfer between the wall and smoke layer, which leads to the decreasing of maximum temperature (Hu, 2006).

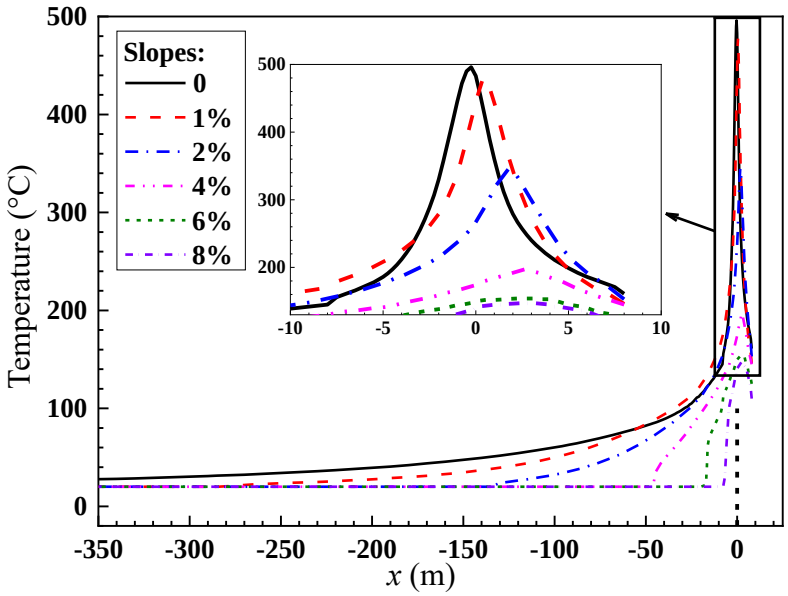

(a) Maximum temperature along the longitudinal centerline

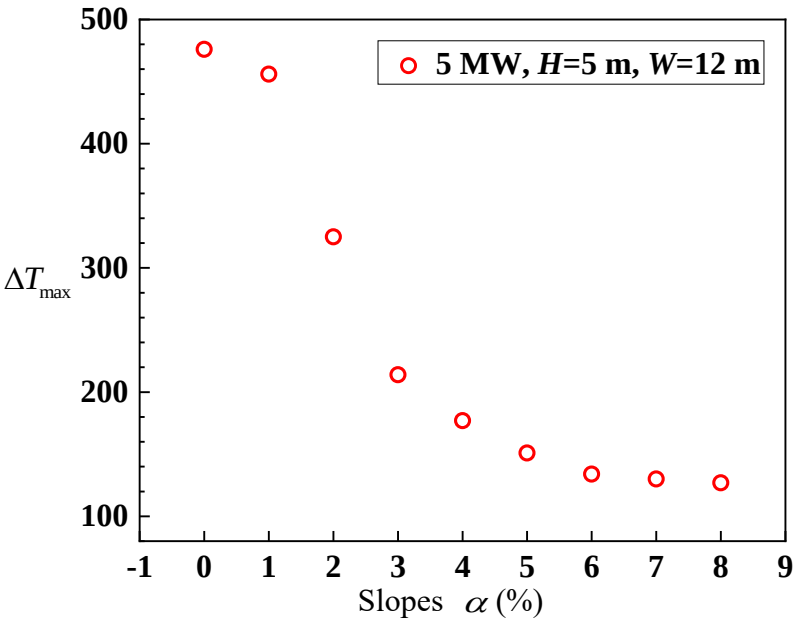

(b) Maximum temperature rise

Fig. 4: Maximum plume temperature rise under the ceiling of various tunnel slopes for $\dot{Q}$ = 5MW, W =12m, H =5m.

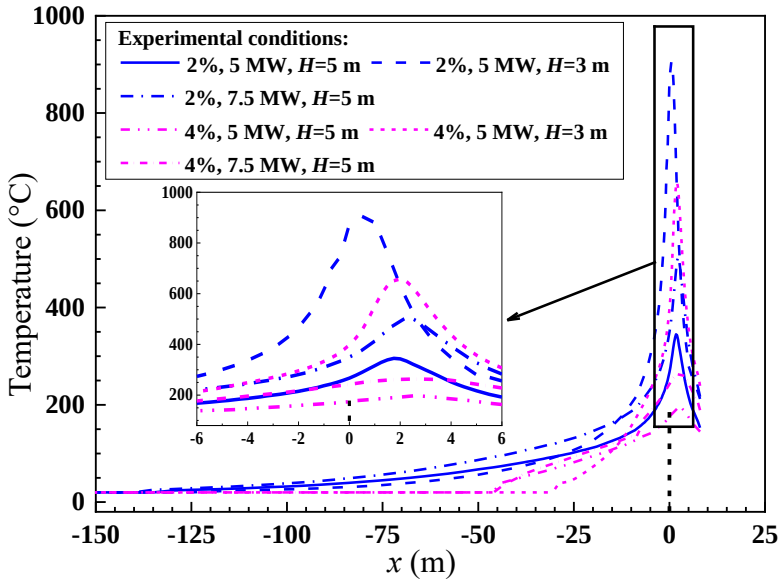

(a) Maximum temperature along the longitudinal centerline

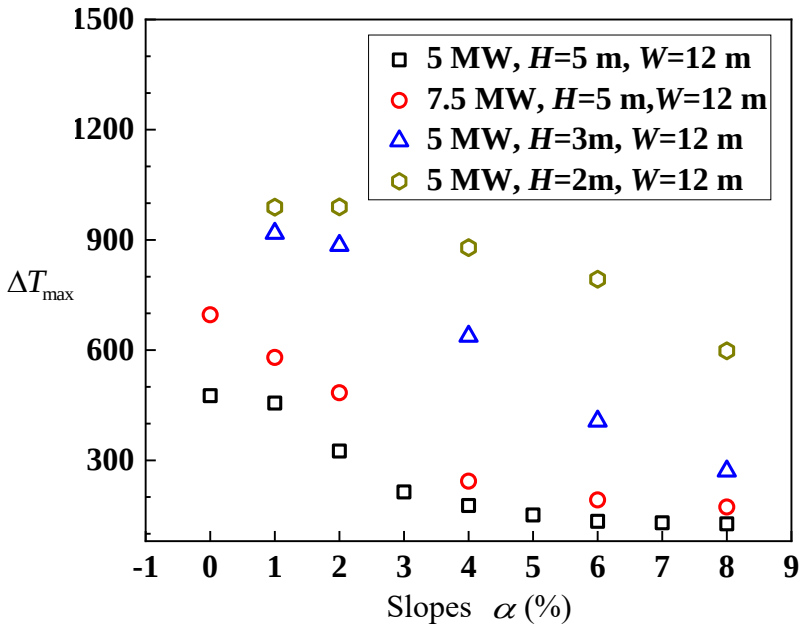

(b) Maximum temperature rise

Fig. 5: Maximum plume temperature rise under the ceiling of various heat release rates and source-ceiling heights for *W*=12 m.

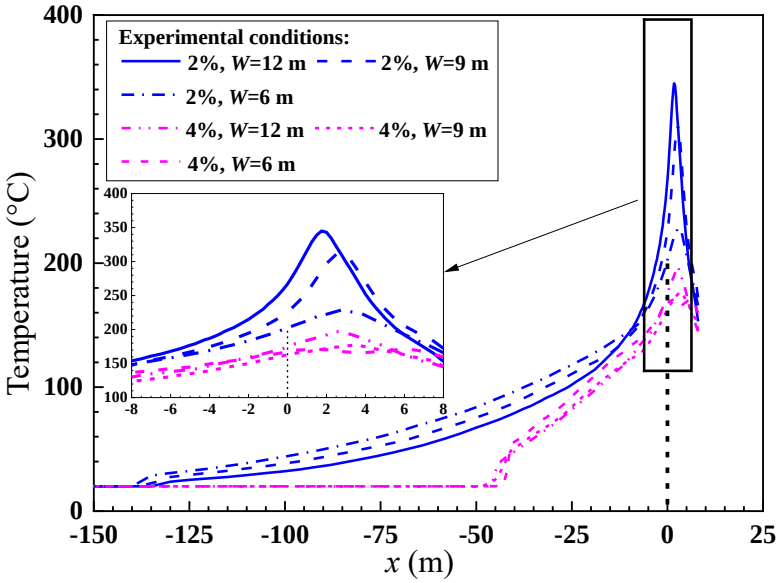

(a) Maximum temperature along the longitudinal centerline

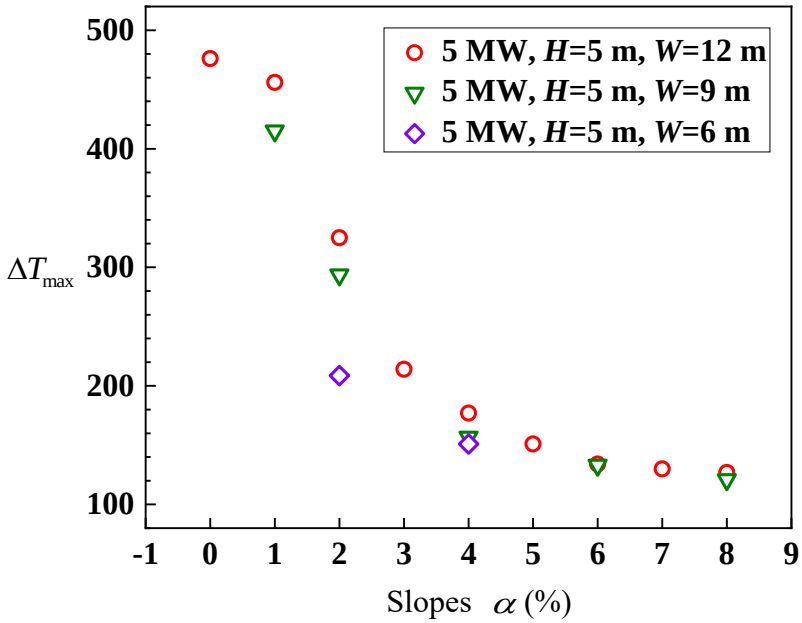

(b) Maximum temperature rise

Fig. 6: Maximum temperature rise under the ceiling of various tunnel widths for $\dot{Q}=5\text{MW}$, $H=5\text{m}$.

Equation (3) shows that the dimensionless temperature rise $\frac{\Delta T_{\max}}{\Delta T_{\max,0}}$ (where $\Delta T_{\max,0}$ is the maximum temperature rise of a horizontal tunnel, i.e., zero tunnel slope) is proportional to tunnel slope. In Fig. 7, we further plot $\frac{\Delta T_{\max}}{\Delta T_{\max,0}}$ against the tunnel slope for the same tunnel width (W=12m) and source-ceiling height (H=5m) but two heat release rates (5 and 7.5 MW). It shows that $\frac{\Delta T_{\max}}{\Delta T_{\max,0}}$ has the following relationship with the tunnel slope:

$$\frac{\Delta T_{\max}}{\Delta T_{\max,0}}=0.73\exp\left(-0.13\alpha^2\right)+0.27,\quad \alpha\le 8 \tag{6}$$

It is noted that, only the effect of heat release rate (with same tunnel width and source-ceiling height) on the non-dimensional maximum temperature rise $\Delta T_{\max}/\Delta T_{\max,0}$ is examined in Fig. 7. Equation (6) shows that the heat release rate has no effect on the non-dimensional maximum temperature rise (the effect of heat release rate on the maximum temperature rise is included in $\Delta T_{\max,0}$). More work is needed for various tunnel width and source-ceiling height to validate Eq. (6).

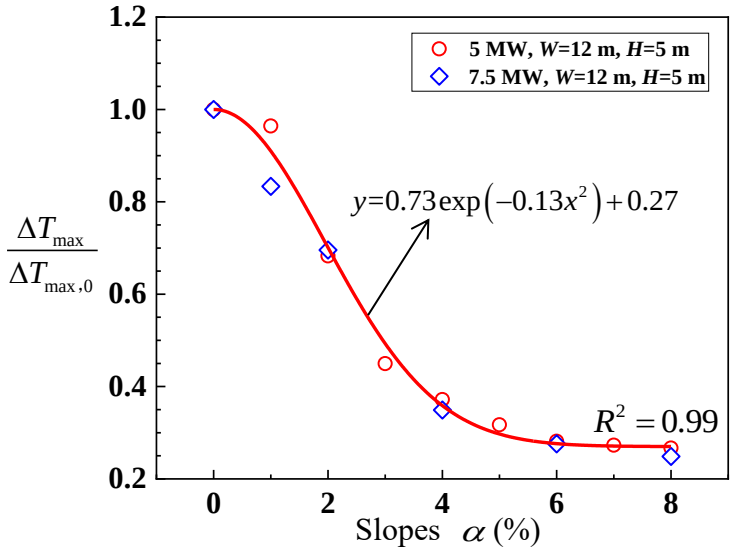

Fig. 7: Non-dimensional maximum temperature rise under the ceiling of various tunnel slopes for $\dot{Q}$ = 5MW, W =12m, H =5m and $\dot{Q}$ = 7.5MW, W =12m, H =5m.

3.2 Smoke back-layering lengths

Figure 8 shows the smoke spread of various tunnel slopes for $\dot{Q}$ = 5MW, H =5m, W = 12m at the steady spread state. It can be seen that for the horizontal tunnel (tunnel slope α=0), the smoke spread out of the tunnel from both two ends. With the increasing of the tunnel slope, the smoke stagnates at a distance from the fire source due to the stack effect in the downhill direction from the fire source, and the smoke back-layering length (S) in this direction decreases with the increasing of the tunnel slope as shown in Fig. 8. This is because that the increasing tunnel slope increases the stack effect.

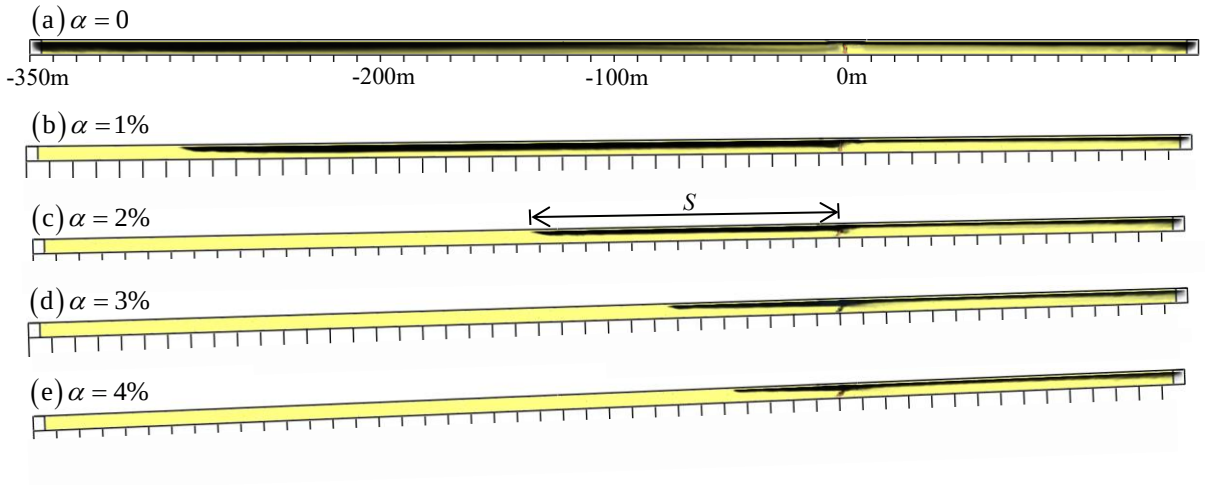

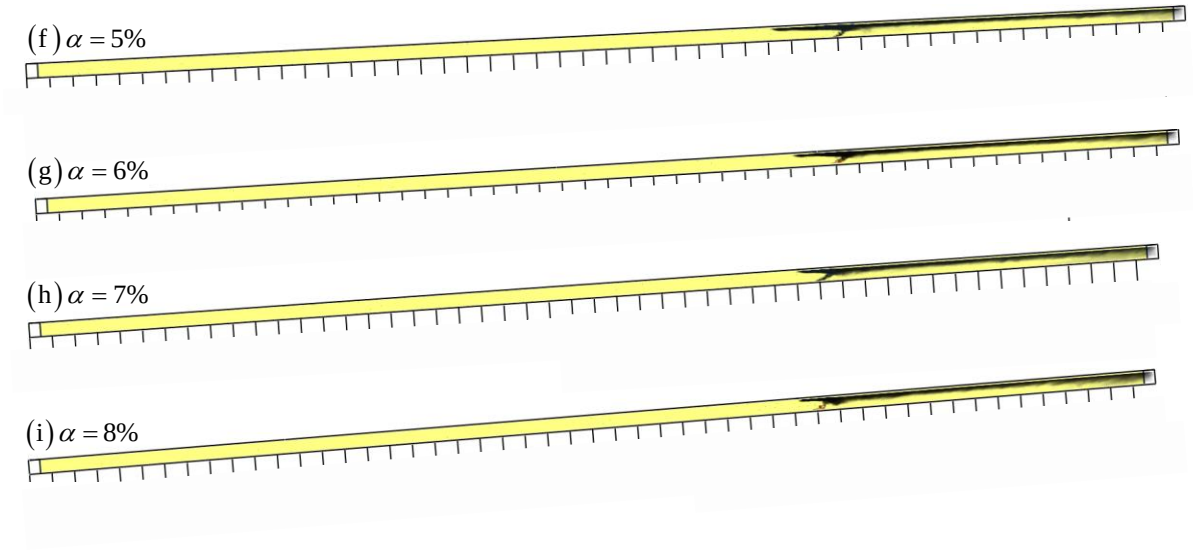

Fig. 8: Smoke spread of various tunnel slopes with $\dot{Q} = 5$MW, H=5m, W = 12m.

Figure 9 shows the smoke spread of various heat release rates for tunnel slopes of 1%, 2%, 4%, 6% and 8% with a source-ceiling height of 5 m. The comparisons between two heat release rates in Fig. 9 show that for a given tunnel slope, source-ceiling height and tunnel width, the heat release rate has no significant effect on the smoke back-layering length, especially for large tunnel slope. In (Ji *et al.*, 2015), numerical studies on the smoke spread of a tilted tunnel with tunnel length of 60 m and slopes of 5% ~ 15% were conducted, and their results (Figs. 4 and 6 in Ji *et al.*, 2015) also showed that the heat release rate had no significant effect on the smoke back-layering length (in Ji *et al.*, 2015, S was defined as the horizontal distance at the centerline from the fire source to the location with sharp temperature decrease).

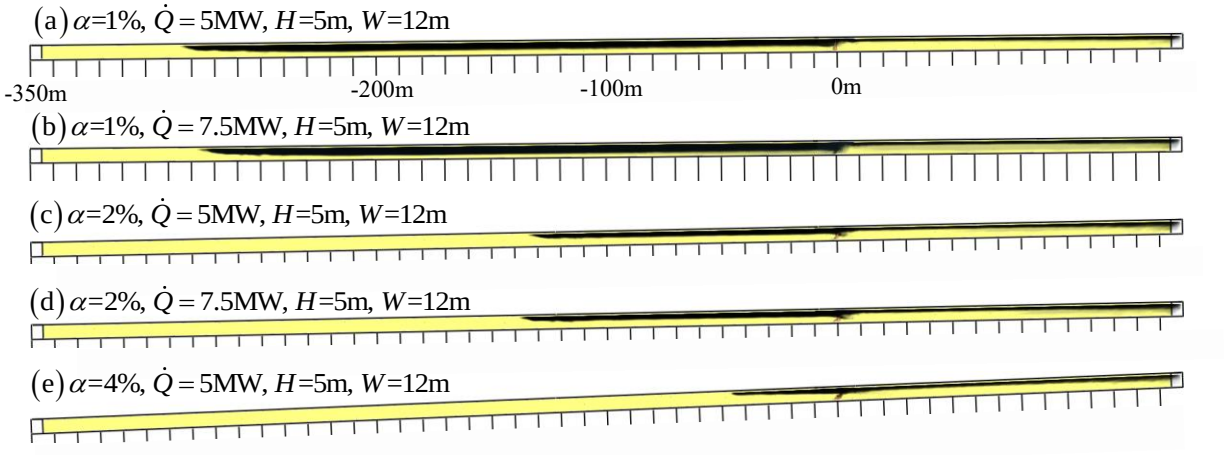

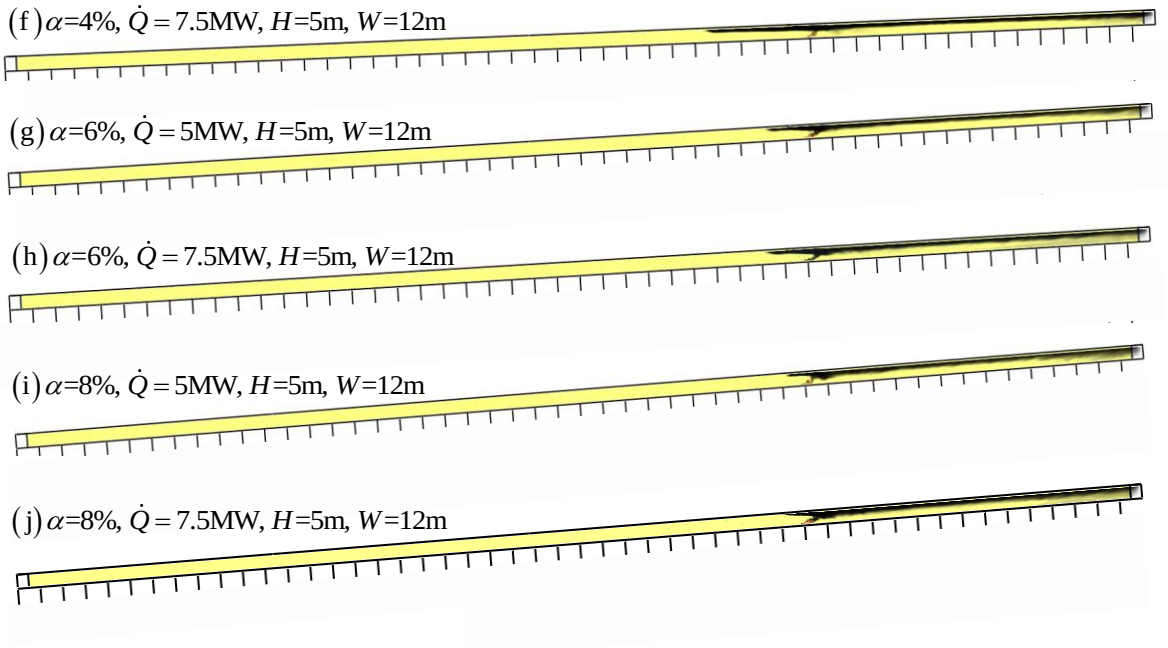

Fig. 9: Effect of heat release rate on the smoke back-layering length.

Then, we further considering the effect of the source-ceiling height H on the smoke back-layering length. Figure 10 shows the smoke spread of various source-ceiling heights for tunnel slopes of 1%, 2%, 4%, 6% and 8% with a heat release rate of 5 MW and a tunnel width of 12 m. The comparisons between different source-ceiling heights in Fig. 10 show that for a given tunnel slope, heat release rate and tunnel width, the smoke back-layering length decreases with the decreasing of the source-ceiling height.

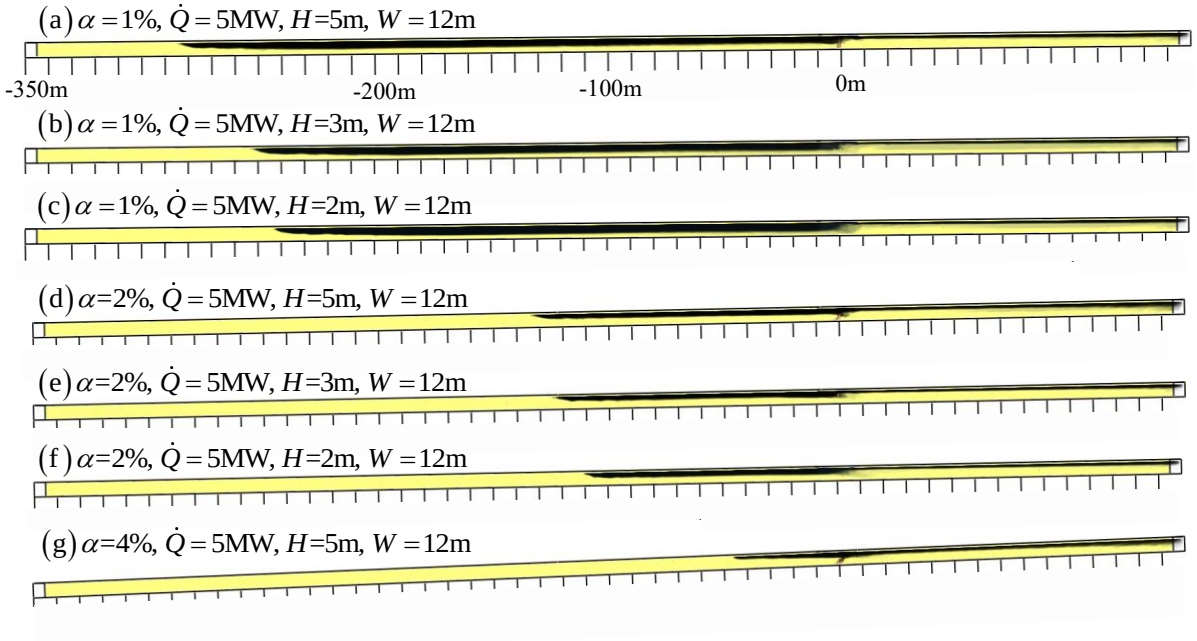

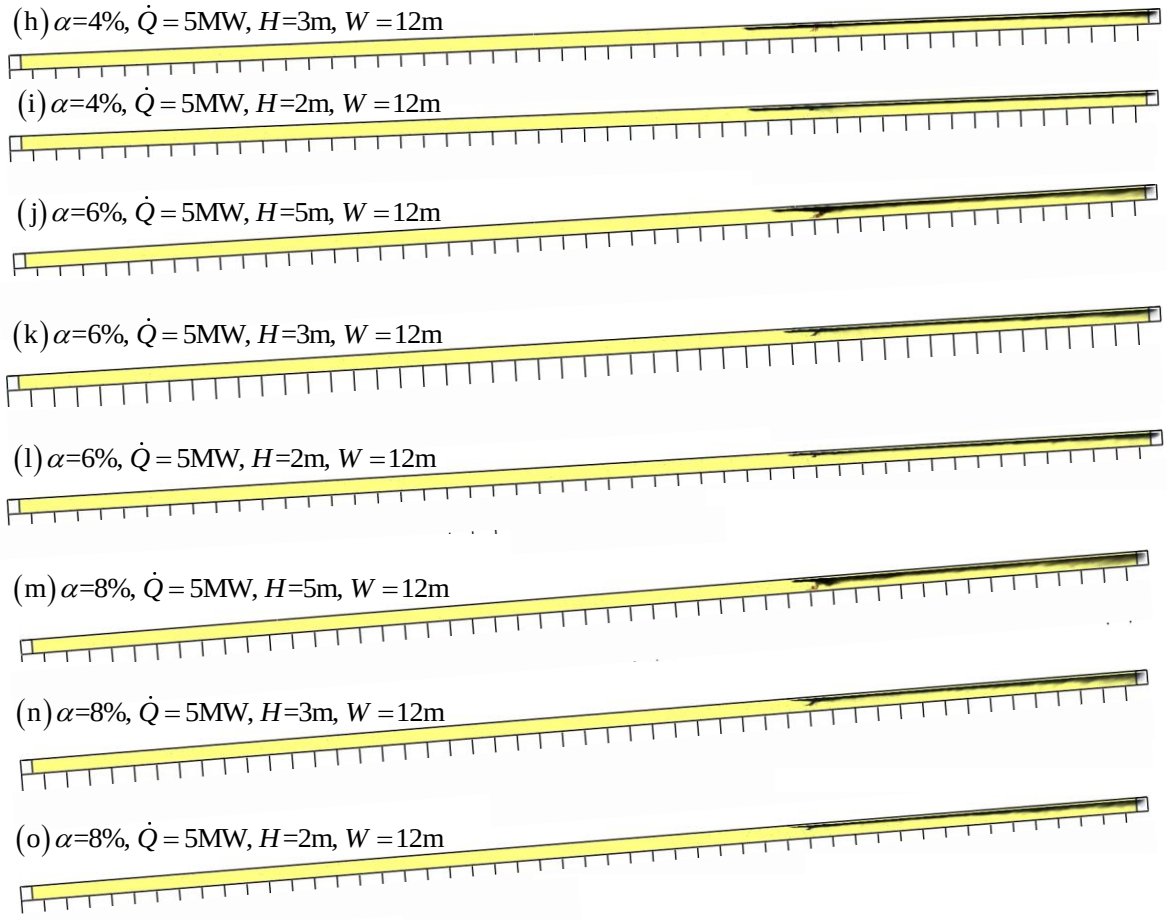

Fig. 10: Effect of source-ceiling height on the smoke back-layering length.

Figure 11 shows the smoke spread of various tunnel widths for tunnel slopes of 1%, 2%, 4%, 6% and 8% with heat release rate of 5 MW and source-ceiling height of 5 m. From Fig. 11, we can see that the tunnel width has no significant effect on the smoke back-layering length *S*, especially for large tunnel slope. The results in Wang *et al.*, 2020 show that the air flow velocity induced by the stack effect hold almost constant with the tunnel width. Therefore, the tunnel width has no significant effect on *S*.

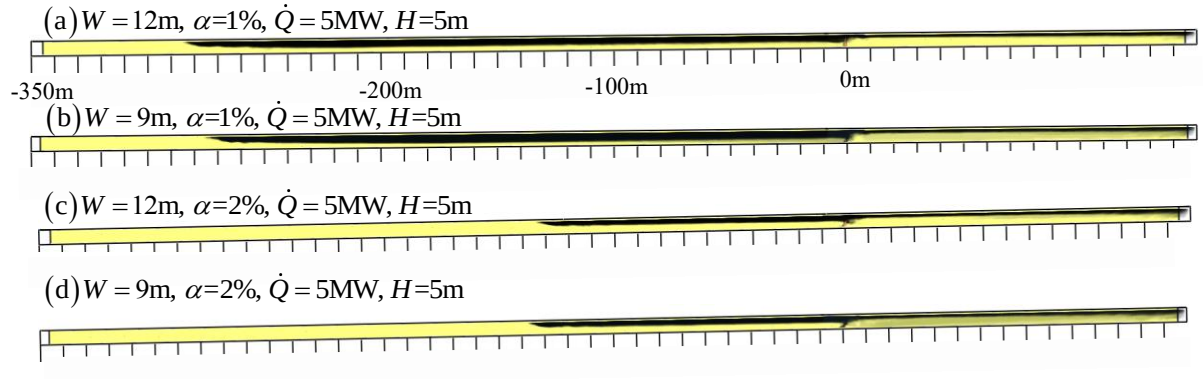

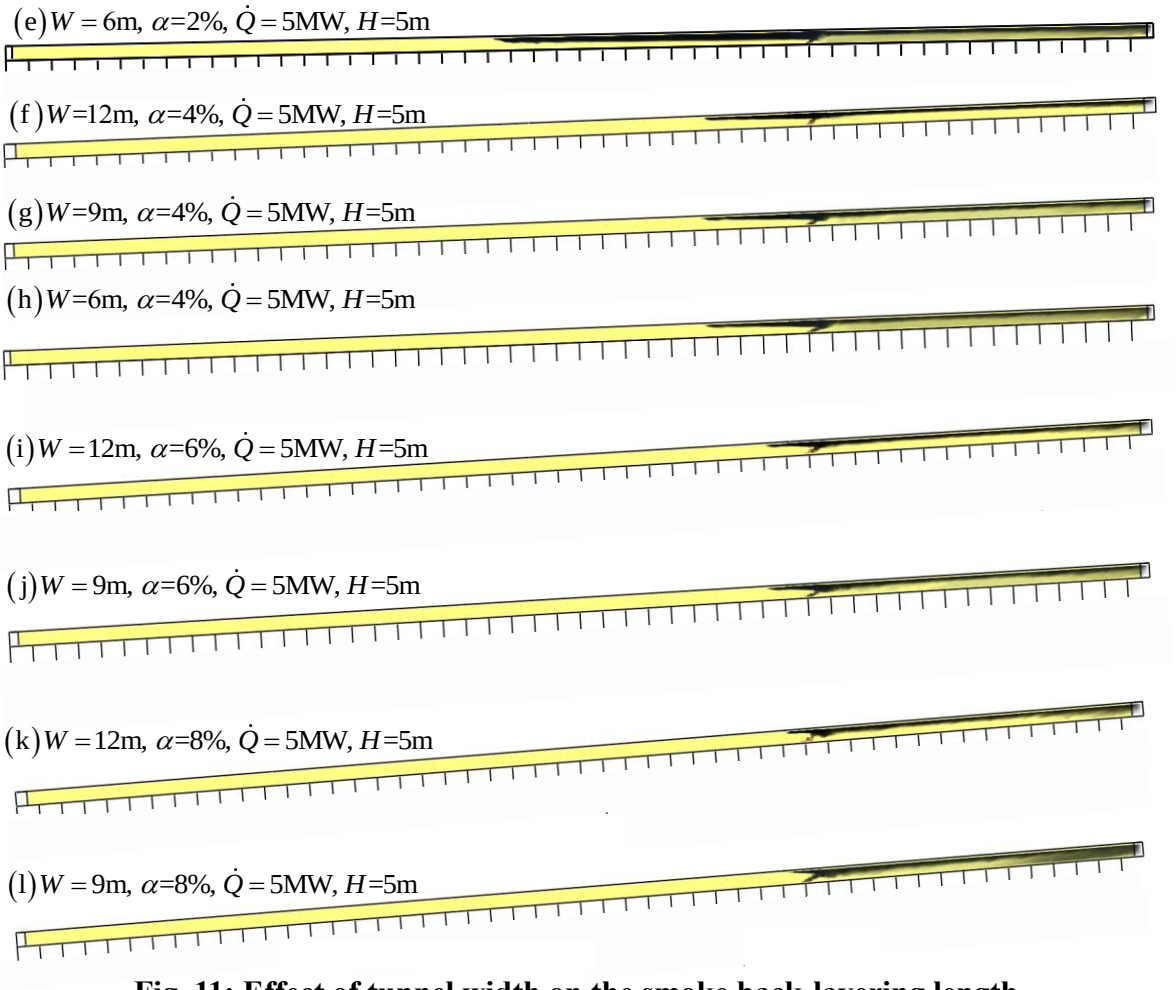

Fig. 11: Effect of tunnel width on the smoke back-layering length.

Then, the averaged smoke back-layering lengthes at the smoke steady spread state are obtained from smokeview results for all the numerical simulation cases as shown in Fig. 12.

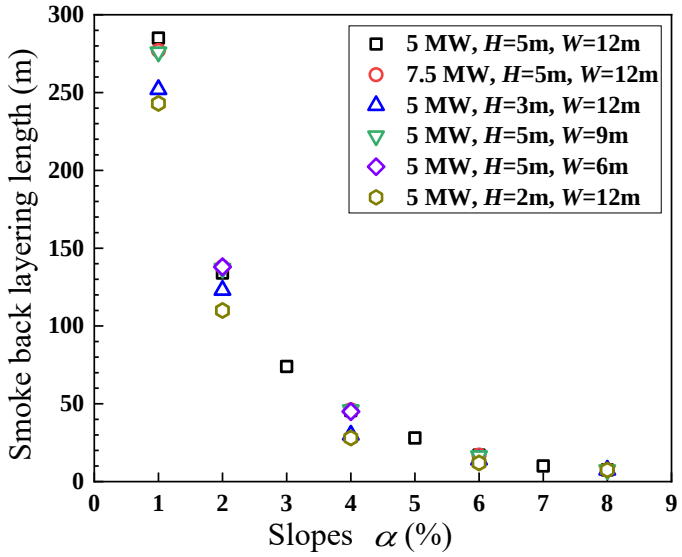

Fig. 12: Smoke back layering lengths of various tunnel slopes (α), heat release rates ($\dot{Q}$), source-ceiling heights (H) and tunnel widths (W).

3.3 Prediction model of smoke back-layering length in a tilted tunnel

The smoke back-layering length in a tilted tunnel is mainly determined by the stack effect and the static pressure difference. Neglecting the internal friction with the ceiling, stack effect caused by the temperature difference between the smoke layer and air gives the following equation in a tilted tunnel (Chow *et al.*, 2015, 2016)

$$\Delta P_{stack} = \cos\theta \int_r^S (\rho_\infty - \rho_x) g \alpha \mathrm{d}x \tag{7}$$

where $\theta = arctan\alpha$, S is the smoke back-layering length along the tunnel in a tilted tunnel, r is the location of the reference point， α is the tunnel slope defined as the ratio of uphill height to horizontal length of tunnel， ρ_∞ is the ambient air density, ρ_x is the mean density of the transverse section at the distance x from the reference point. The static pressure difference given by the density difference between ambient air and the smoke $\Delta\rho_S$ and the thickness of the smoke layer h at the stagnation point can be expressed as (Chow *et al.*, 2015; Wang *et al.*, 2016)

$$\Delta P_{static} = \frac{1}{2} \Delta\rho_S g h \tag{8}$$

In the downhill direction from the fire source of a tilted tunnel, the static pressure difference ΔP_{static} is the driving force of the smoke movement, however, the stack effect ΔP_{stack} is against the direction of smoke movement. At the smoke stagnation point for a tilted tunnel under natural ventilation, static pressure ΔP_{static} has to be equal to the pressure difference caused by stack effect ΔP_{stack} (Chow *et al.*, 2015; 2016)

$$\Delta P_{static} = \Delta P_{stack} \tag{9}$$

From the ideal gas law (Wang et al., 2016; Chow *et al.*, 2016), we have

$$\frac{\rho_x}{\rho_\infty} = \frac{T_\infty}{T_x} \tag{10}$$

where T_x is the mean temperature of the transverse section at the distance x from the reference point. Equation (7) can be rearranged as

$$\Delta P_{stack} = \cos\theta \int_r^S \rho_\infty \left(1 - \frac{T_\infty}{T_x}\right) g\alpha \mathrm{d}x = \cos\theta \int_r^S \rho_\infty \left(1 - \frac{T_\infty}{\Delta T_x + T_\infty}\right) g\alpha \mathrm{d}x \tag{11}$$

The location of the smoke stagnation point depends on the temperature difference ΔT_x. For the static pressure difference,

$$\Delta P_{static} = \frac{1}{2}\Delta\rho_S gh = \frac{1}{2}\left(\rho_\infty - \rho_S\right) gh = \frac{1}{2}\left(\rho_\infty - \rho_\infty \frac{T_\infty}{T_S}\right) gh = \frac{1}{2}\rho_\infty gh \frac{\Delta T_S}{T_S} \tag{12}$$

where ρ_S is the smoke density at the smoke stagnation point, T_S is the smoke temperature at the smoke stagnation point. Then, we have

$$\cos\theta \int_r^S \rho_\infty \left(1 - \frac{T_\infty}{\Delta T_x + T_\infty}\right) g\alpha \mathrm{d}x = \frac{1}{2}\rho_\infty gh \frac{\Delta T_S}{T_S} \tag{13}$$

Equation (13) shows that the temperature decay profile and the smoke thickness at the smoke stagnation point are required to predict the smoke back-layering length in the downhill direction from the fire source of a tilted tunnel. The temperature decay profile is related to the heat release rate, the source-ceiling height and the dimensions of the tunnel (Zhang *et al.*, 2014, 2019). However, to the best knowledge of the authors, no research has been done on the two parameters for a strong fire plume (with large heat release rate) in a tilted tunnel (Chen *et al.*, 2018). Next, we propose a semi-empirical model for the smoke back-layering length based on dimensional analysis.

According to the above analysis (Eqs. (7)-(13)), the most important parameters controlling the smoke back-layering length are heat release rate $\dot{Q}$, tunnel width W, tunnel length L_t, tunnel height H_t (5 m in this study), source-ceiling height H (distance between the fire source exit and the ceiling, 2 m, 3 m and 5 m in this study as shown in Table 1), air density ρ_∞, gravity acceleration g, specific heat of air c_p, ambient air temperature T_∞ and the tunnel slop α. In this work, the tunnel length has

a constant value of 500 m. So, it is not included in the following dimensional analysis. The above parameters have the dimensions as $\dot{Q}$ [ML^2T^{-3}], W [L], H_t [L], H [L], ρ_∞ [ML^{-3}], g [LT^{-2}], c_p [$L^2T^{-2}\Theta^{-1}$], T_∞ [Θ] and α [-], accordingly. Then, we have the following function

$$f\left(\dot{Q}, W, H_t, H, \rho, g, c_p, T, \alpha, S\right) = 0 \tag{14}$$

Here we take H, ρ_∞, c_p and g as the fundamental quantities. Then six dimensionless quantities are obtained as $\Pi_1 = \frac{\dot{Q}}{H^{a1}\rho_\infty{}^{b1}c_p{}^{c1}g^{d1}}$, $\Pi_2 = \frac{W}{H^{a2}\rho_\infty{}^{b2}c_p{}^{c2}g^{d2}}$, $\Pi_3 = \frac{H_t}{H^{a3}\rho_\infty{}^{b3}c_p{}^{c3}g^{d3}}$ $\Pi_4 = \frac{S}{H^{a4}\rho_\infty{}^{b4}c_p{}^{c4}g^{d4}}$, $\Pi_5 = \frac{T_\infty}{H^{a5}\rho_\infty{}^{b5}c_p{}^{c5}g^{d5}}$, $\Pi_6 = \alpha$. Based on the Principle of Dimensional Homogeneity, we have

$$\left[ML^2T^{-3}\right] = \left[L\right]^{a1}\left[ML^{-3}\right]^{b1}\left[L^2T^{-2}\Theta^{-1}\right]^{c1}\left[LT^{-2}\right]^{d1} \tag{15a}$$

$$\left[L\right] = \left[L\right]^{a2}\left[ML^{-3}\right]^{b2}\left[L^2T^{-2}\Theta^{-1}\right]^{c2}\left[LT^{-2}\right]^{d2} \tag{15b}$$

$$\left[L\right] = \left[L\right]^{a3}\left[ML^{-3}\right]^{b3}\left[L^2T^{-2}\Theta^{-1}\right]^{c3}\left[LT^{-2}\right]^{d3} \tag{15c}$$

$$\left[L\right] = \left[L\right]^{a4}\left[ML^{-3}\right]^{b4}\left[L^2T^{-2}\Theta^{-1}\right]^{c4}\left[LT^{-2}\right]^{d4} \tag{15d}$$

$$\left[\Theta\right] = \left[L\right]^{a5}\left[ML^{-3}\right]^{b5}\left[L^2T^{-2}\Theta^{-1}\right]^{c5}\left[LT^{-2}\right]^{d5} \tag{15e}$$

According to Eq. (15), $a1$=7/2, $b1$=1, $c1$=0, $d1$=3/2; $a2$=1, $b2$=0, $c2$=0, $d2$=0; $a3$=1, $b3$=0, $c3$=0, $d3$=0; $a4$=1, $b4$=0, $c4$=0, $d4$=0; $a5$=1, $b5$=0, $c5$=-1, $d5$=1. Then Eq. (14) is rearranged as

$$\frac{S}{H} = f\left(\frac{\dot{Q}}{H^{7/2}\rho_\infty g^{3/2}}, \frac{W}{H}, \frac{H_t}{H}, \frac{T_\infty}{Hc_p{}^{-1}g}, \alpha\right) \tag{16}$$

Eq. (16) can be further rearranged as

$$\frac{S}{H} = f\left(\frac{\dot{Q}}{H^{7/2}\rho_\infty g^{3/2}}, \frac{W}{H_t}, \frac{T_\infty}{Hc_p{}^{-1}g}, \alpha\right) \tag{17}$$

According to the numerical results (Figs. 9 and 11), heat release rate and tunnel width have no significant effect on the smoke back-layering length. So, for the smoke back-layering length, we have

$$\frac{S}{H}=\left(\frac{T_\infty}{Hc_p^{-1}g}\right)^k f(\alpha) \tag{18}$$

Since the smoke back-layering length decreases with the decreasing of the source-ceiling height H as shown in Fig. 10, k is a constant smaller than 1. However, the form of $f(\alpha)$ is still unknown.

In order to propose the correlation for smoke back-layering length, the numerical simulation results are used and the constant k is found to be 0.7, which is valid for all the data for the same tunnel slope as shown in Fig. 13. Then a correlation for the smoke back-layering length in the downhill direction from the fire source of a tilted tunnel is proposed as shown in Eq. (19)

$$\frac{S}{H}=\left(\frac{T_\infty}{Hc_p^{-1}g}\right)^{0.7}\left(0.33+31.52\cdot 0.5^{\alpha}\right),\quad \alpha\le 8 \tag{19}$$

To validate Eq. (19), the calculated smoke back-layering lengths using Eq. (19) are compared to the simulated smock back-layering lengths and the comparison results are shown in Fig. 14. It can be seen that in Fig. 14 that Eq. (19) can predict the smoke back-layering lengths well.

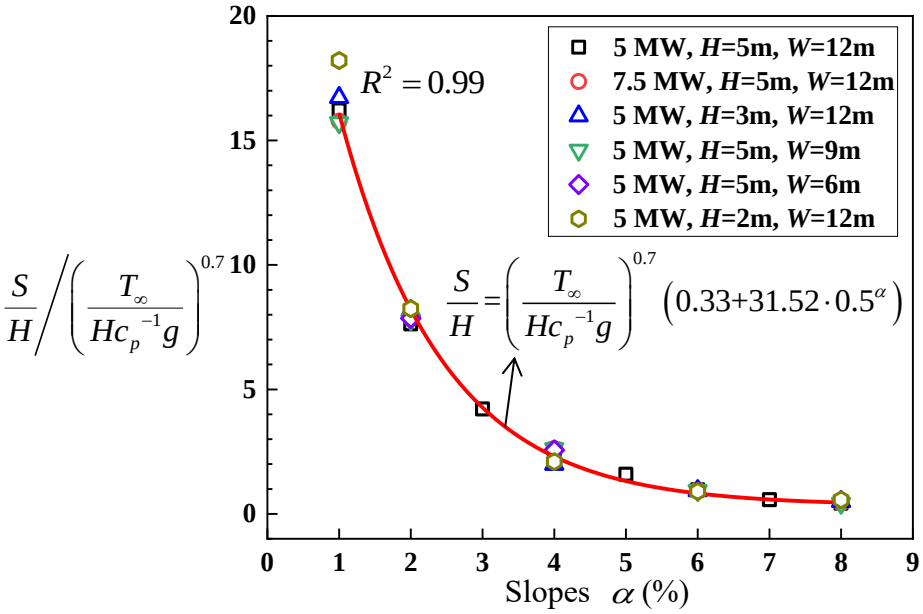

Fig. 13: Correlation for the smoke back layering lengths of various tunnel slopes, heat release rates, source-ceiling heights and tunnel widths.

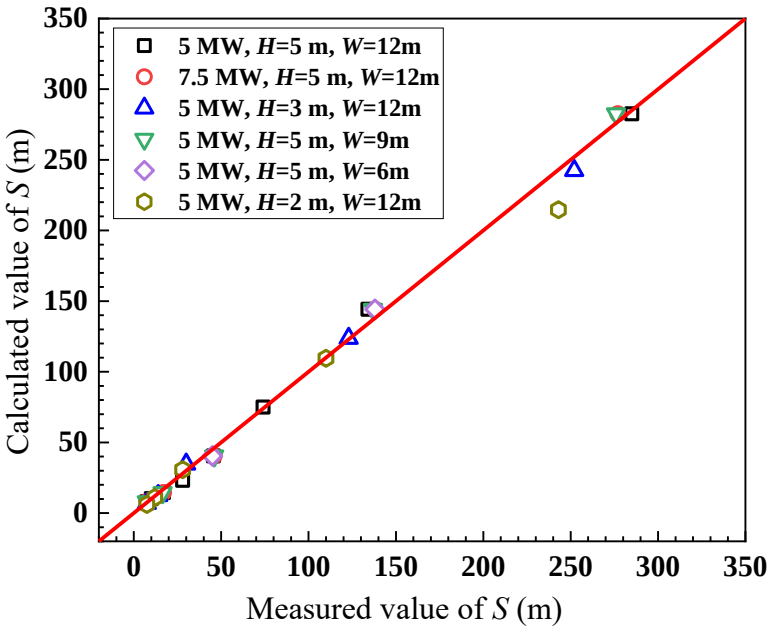

Fig. 14: Comparison of numerically measured values of *S* with the predictions by Eq. (19).

It is noted that Eq. (19) is applicable for the numerical conditions of this study, i.e. heat release rates of 5 MW ~ 7.5 MW, source ceiling heights of 2 m ~ 5 m, tunnel widths of 6 m ~ 12 m and tunnel slopes of 1% ~ 8%. We can imagine that for very large tunnel slope, there would be no smoke back-layering length. It is necessary to investigate larger tunnel slopes in the future. At the same time, another very important parameter for the smoke back-layering length in a tilted tunnel is the tunnel length L_t which has significant effect on the stack effect. However, in this work, only one tunnel length is considered, and as a result the tunnel length is not included in Eq. (19). It would be an interesting and important future work to extend Eq. (19) to various tunnel lengths.

4. Conclusions

This paper investigates numerically the maximum temperature and smoke back-layering length in the downhill direction from a fire source in a tilted tunnel under natural ventilation by using FDS. Major findings include:

(1) The maximum temperature under the ceiling of tilted tunnel decreases with the increasing of

tunnel slope or the decreasing of tunnel width. However, it increases with the increasing of heat release rate or the decreasing of source-ceiling height. A model was proposed for the maximum temperature rise (Eq. (6)).

(2) The smoke back-layering length decreases with the increasing of the tunnel slope (Fig. 8). Fire source heat release rate and tunnel width have no significant effect on the smoke back-layering length (Figs. 9 and 11). And the smoke back-layering length decreases with the decreasing of source-ceiling height (Fig. 10).

(3) Based on dimensional analysis, a simple model, which includes the effects of the tunnel slope α and source-ceiling height H, is proposed to correlate the data of this study (Fig. 13; Eq. (19)).

Acknowledgements

This work was funded jointly by National Natural Science Foundation of China (NSFC) under Grant no. 51906240, Opening Funds of State Key Laboratory of Building Safety and Built Environment and National Engineering Research Center of Building Technology under Grant no. BSBE2018-05, National Natural Science Foundation of China (NSFC) under Grant no. 51776060, and China Postdoctoral Science Foundation under Grant no. 2019M652213.

Reference

Atkinson, G.T., Wu,Y., 1996. Smoke control in sloping tunnels. *Fire Safety J.* 27, 335-341.

Chen, L.F., Hu, L.H., Tang, W., Yi, L., 2013. Studies on buoyancy driven two-directional smoke flow layering length with combination of point extraction and longitudinal ventilation in tunnel fires. *Fire Safety J.* 59, 94-101.

Chen, L.F., Hu, L.H., Zhang, X.L., Zhang, X.Z., Zhang, X.C., Yang, L.Z., 2015. Thermal buoyant

smoke back-layering flow length in a longitudinal ventilated tunnel with ceiling extraction at difference distance from heat source. *Appl. Therm. Eng.* 78, 129-135.

Chen, L., Tang, F., Wang, Q., Li, L.J., 2018. Experimental study on temperature distribution of ceiling jet in tunnel fires under natural ventilation. *Procedia Eng.* 211, 674-680.

Chen, C.K., Nie, Y.L., Zhang, Y.L., Lei, P., Fan, C.G., Wang, Z.Y., 2020. Experimental investigation on the influence of ramp slope on fire behaviors in a bifurcated tunnel. *Tunn. Undergr. Sp. Tech.* 104, 103522.

Chen, C.K., Zhang, Y.L., Lei, P., Jiao, W.B., 2020. A study for predicting the maximum gas temperature beneath ceiling in sealing tactics against tunnel fire. *Tunn. Undergr. Sp. Tech.* 98, 103275.

Chow, W.K., Gao, Y., Zhao, J.H., Dang, J.F., Chow, C.L., Miao, L., 2015. Smoke movement in tilted tunnel fires with longitudinal ventilation. *Fire Safety J.* 75, 14-22.

Chow, W.K., Gao, Y., Zhao, J.H., Dang, J.F., Chow, Nadia C.L., 2016. A study on tilted tunnel fire under natural ventilation. *Fire Safety J.* 81, 44-57.

Fire Dynamics Simulator User's Guide, NIST Special Publication 1019 Sixth Edition.

Harish, R., Venhatasubbaiah, K., 2014. Effects of buoyancy induced roof ventilation systems for smoke removal in tunnel fires. *Tunn. Undergr. Sp. Tech.* 42, 195-205.

Hu, L.H., 2006. Studies on Thermal Physics of Smoke Movement in Tunnel Fires (Ph.D. thesis). Hefei: University of Science and Technology of China.

Hu, L.H., 2017. A review of physics and correlations of pool fire behaviour in wind and future challenges. *Fire Safety J.* 91, 41-55.

Hu, L.H., Chen, L.F., Wu, L., Li, Y.F., Zhang, J.Y., Meng, N., 2013. An experimental investigation

and correlation on buoyant gas temperature below ceiling in a slopping tunnel fire. *Appl. Therm. Eng.* 51, 246-254.

Hu, L.H., Huo, R., Chow, W.K., 2008. Studies on buoyancy-driven back-layering flow in tunnel fires. *Exp. Therm. Fluid Sci.* 32 (8), 1468-1483.

Hu, L.H., Huo, R., Li, Y.Z., Wang, H.B., Chow, W.K., 2005. Full-scale burning tests on studying smoke temperature and velocity along a corridor. *Tunn. Undergr. Sp. Tech.* 20, 223-229.

Hu, L.H., Huo, R., Peng, W., Chow, W.K., Yang, R.X., 2003. On the maximum smoke temperature under the ceiling in tunnel fires. *Tunn. Undergr. Sp. Tech.* 21, 650-655.

Hu, L.H., Huo, R., Wang, H.B., Li, Y.Z., Yang, R.X., 2007. Experimental studies on fire induced buoyant smoke temperature distribution along tunnel ceiling. *Build. Environ.* 42 (11), 3905-3915.

Ji, J., Wan, H.X., Li, K.Y., Han, J.Y., Sun, J.H., 2015. A numerical study on upstream maximum temperature in inclined urban road tunnel fires. *Int. J. Heat Mass Tran.* 88, 516-526.

Ko, J., Yoon, C., Yoon, S., Kim, J., 2010. Determination of the applicable exhaust airflow rate through a ventilation shaft in the case of road tunnel fires. *Safety Sci.* 48, 722-728.

Kurioka, H., Oka, Y., Satoh, H., Sugawa, O., 2003. Fire properties in near field of square fire source with longitudinal ventilation in tunnels. *Fire Safety J.* 38 (4), 319-340.

Li, Y.Z., Lei, B., Ingason, H., 2010. Study of critical velocity and backlayering length in longitudinally ventilated tunnel fires. *Fire Safety J.* 45, 361-370.

Li, Y.Z., Lei, B., Ingason, H., 2011. The maximum temperature of buoyancy-driven smoke flow beneath the ceiling in tunnel fires. *Fire Safety J.* 46, 204-210.

Li, Y.Z., Ingason, H., 2012. The maximum ceiling gas temperature in a large tunnel fire. *Fire Safety J.* 48, 38-48.

Meng, N., Hu, L.H., Wu, L., Yang, L.Z., Zhu, S., Chen, L.F., Tang, W., 2014. Numerical study on the optimization of smoke ventilation mode at the conjunction area between tunnel track and platform in emergency of a train fire at subway station. *Tunn. Undergr. Sp. Tech.* 40, 151-159.

Oka, Y., Kakae, N., Imazeki, O., Inagaki, K., 2013. Temperature property of ceiling jet in an inclined tunnel. *Procedia Eng.* 62, 234-241.

Shafee, S., Yozgatligil, A., 2018. An analysis of tunnel fire characteristics under the effects of vehicular blockage and tunnel inclination. *Tunn. Undergr. Sp. Tech.* 79, 274-285.

Tang, W., Hu, L.H., Chen, L.F., 2013. Effect of blockage-fire distance on buoyancy driven back-layering length and critical velocity in a tunnel: An experimental investigation and global correlations. *Appl. Therm. Eng.* 60, 7-14.

Tang, F., Hu, L.H., Yang, L.Z., Qiu, Z.W., Zhang, X.C., 2014. Longitudinal distributions of CO concentration and temperature in buoyant tunnel fire smoke flow in a reduced pressure atmosphere with lower air entrainment at high altitude. *Int. J. Heat Mass Tran.* 75, 130-134.

Wang, Z.Y., Ding, L., Wan, H.X., Ji, J., Gao, Z.H., Yu, L.X., 2020. Numerical investigation on the effect of tunnel width and slope on ceiling gas temperature in inclined tunnels. *Int. J. Therm. Sci.* 152, 106272.

Wang, Y.F., Sun, X.F., Liu, S., Yan, P.N., Qin, T., Zhang, B., 2016. Simulation of back-layering length in tunnel fire with vertical shafts. *Appl. Therm. Eng.* 109, 344-350.

Wang, Z.L., Zhu, L., Guo, X.X., Pan, X.H., Zhou, B., Yang, J., Jiang, J.C., Hua, M., Feng, L., 2019. Reduced-scale experimental and numerical study of fire in a hybrid ventilation system in a large underground subway depot with superstructures under fire scenario. *Tunn. Undergr. Sp. Tech.* 88, 98-112.

Weng, M.C., Lu, X.L., Liu, F., Du, C.X., 2016. Study on the critical velocity in a sloping tunnel fire under longitudinal ventilation. *Appl. Therm. Eng.* 94, 422-434.

Wu, Y.J., Stoddard, J.P., James, P., Atkinson, G.T., 1997. Effect of slope on control of smoke flow in tunnel fires, *Fire Safety Science-Proceedings of the Fifth International Symposium*, 1225-1236.

Zhang, X.C., Hu, L.H., Zhu, W., Zhang, X.L., Yang, L.Z., 2014. Flame extension length and temperature profile in thermal impinging flow of buoyant round jet upon a horizontal plate. *Appl. Therm. Eng.* 73 (1), 15-22.

Zhang, X.L., Hu, L.H., Sun, X.P., 2019. Temperature profile of thermal flow underneath an inclined ceiling induced by a wall-attached fire. *Int. J. Therm. Sci.* 141, 133-140.

Figure captions

Fig. 1: Physical model of the tilted tunnel and the mesh sizes (top view).

Fig. 2: Validation of the FDS prediction.

Fig. 3: Smoke spread behavior for 7.5 MW, W=12 m, H=5 m and α=2%.

Fig. 4: Maximum plume temperature rise under the ceiling of various tunnel slopes for $\dot{Q}=5\text{MW}$, W=12m, H=5m.

Fig. 5: Maximum plume temperature rise under the ceiling of various heat release rates and source-ceiling heights for W=12 m.

Fig. 6: Maximum plume temperature rise under the ceiling of various tunnel widths for $\dot{Q}=5\text{MW}$, H=5m.

Fig. 7: Non-dimensional maximum temperature rise under the ceiling of various tunnel slopes for $\dot{Q}=5\text{MW}$, W=12m, H=5m and $\dot{Q}=7.5\text{MW}$, W=12m, H=5m.

Fig. 8: Smoke spread of various tunnel slopes with $\dot{Q}=5\text{MW}$, H=5m, $W=12\text{m}$.

Fig. 9: Effect of heat release rate on the smoke back-layering length.

Fig. 10: Effect of source-ceiling height on the smoke back-layering length.

Fig. 11: Effect of tunnel width on the smoke back-layering length.

Fig. 12: Smoke back layering lengths of various tunnel slopes (α), heat release rates ($\dot{Q}$), source-ceiling heights (H) and tunnel widths (W).

Fig. 13: Correlation for the smoke back layering lengths of various tunnel slopes, heat release rates, source-ceiling heights and tunnel widths.

Fig. 14: Comparison of numerically measured values of S with the predictions by Eq. (19).

Table captions

Table 1 Summary of numerical simulation conditions.